

Vibronic Structure in the Room Temperature Photoluminescence of the Halide Perovskite



Kelsey K. Bass,[†] Laura Estergreen,[†] Christopher N. Savory,[‡] John Buckeridge,[‡]
David O. Scanlon,^{‡,¶} Peter I. Djurovich,[†] Stephen E. Bradforth,[†] Mark E.
Thompson,[†] and Brent C. Melot^{*,†}

*Department of Chemistry, University of Southern California, Los Angeles, CA 90089, USA,
University College London, Kathleen Lonsdale Materials Chemistry, 20 Gordon Street, London
WC1H 0AJ, United Kingdom, and Diamond Light Source Ltd., Diamond House, Harwell Science
and Innovation Campus, Didcot, Oxfordshire OX11 0DE, United Kingdom*

E-mail: melot@usc.edu

*To whom correspondence should be addressed

[†]Department of Chemistry, University of Southern California, Los Angeles, CA 90089, USA

[‡]University College London, Kathleen Lonsdale Materials Chemistry, 20 Gordon Street, London WC1H 0AJ, United Kingdom

[¶]Diamond Light Source Ltd., Diamond House, Harwell Science and Innovation Campus, Didcot, Oxfordshire OX11 0DE, United Kingdom

Abstract

We report a study on the optical properties of the layered polymorph of vacancy-ordered triple perovskite $\text{Cs}_3\text{Bi}_2\text{Br}_9$. The electronic structure, determined from Density Functional Theory calculations, shows the top of the valence band and bottom of the conduction band minimum are, unusually, dominated by Bi-*s* and Bi-*p* states respectively. This produces a sharp exciton peak in the absorption spectra with a binding energy that was approximated to be 940 meV, which is substantially stronger than values found in other halide perovskites and, instead, more closely reflects values seen in alkali halide crystals. This large binding energy is indicative of a strongly localized character and results in a highly structured emission at room temperature as the exciton couples to vibrations in the lattice.

Interest in developing new solution processable light-absorbing layers for solar panels has surged since the first reports on the perovskite $\text{CH}_3\text{NH}_3\text{PbI}_3$.¹ Despite the extremely high photovoltaic efficiency these materials have demonstrated,²⁻⁴ the potential environmental and public-health consequences that could result from the wide-scale distribution of solar panels based on water soluble compounds containing Pb presents a huge hurdle to the eventual commercialization of perovskite solar cells.⁵ To address these concerns, perovskites based on Sn^{2+} have been suggested as less-toxic alternatives, but in most cases these analogues have proven too unstable towards oxidation to be realistic replacements.⁶

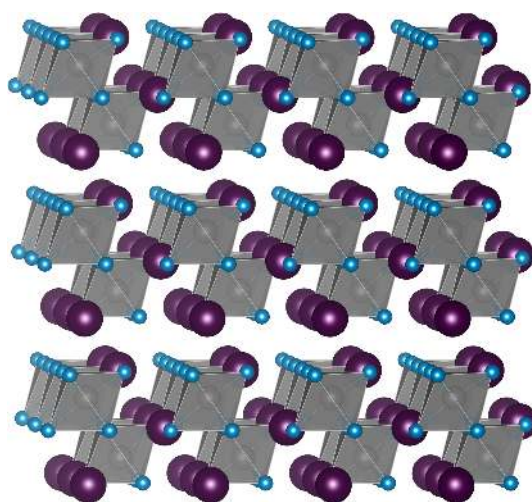


Figure 1: Room temperature crystal structure of $\text{Cs}_3\text{Bi}_2\text{Br}_9$. The gray atoms are Bi, blue atoms are Br, and purple atoms are Cs.

More recently, emphasis has shifted away from maintaining a perfectly isostructural framework towards simply identifying new materials that can efficiently convert sunlight into electrical charge. In this respect, bismuth halides offer a promising new avenue because their strong absorption coefficients make them very effective at capturing the solar spectrum.⁷ Unfortunately, the trivalent oxidation state of Bi ions preclude their direct incorporation into the prototypical ABX_3 perovskite structure. Instead, structural derivatives like double and triple perovskites, which partially substitute some of the bismuth with lower valent metals or vacancies, offer the best opportunity to evaluate the photophysical properties of Bi-based absorbing layers.⁸⁻¹¹

Here, we investigate the optical properties of $\text{Cs}_3\text{Bi}_2\text{Br}_9$, a layered form of the vacancy-ordered

perovskites, which can be viewed as a tripling of the traditional perovskite unit cell with only two thirds of the octahedral positions fully occupied. The remaining octahedral sites remain vacant and segregate so as to produce corrugated layers of corner-sharing BiBr_6 octahedra as illustrated in Figure 1. The resulting local coordination environment of the octahedra is irregular and exhibits a trigonal distortion that produces three short and three long Bi-Br bonds with the shorter linkages shared between neighboring octahedra in each layer.

Previous work on $\text{Cs}_3\text{Bi}_2\text{Br}_9$ found no evidence for photoluminescence above liquid helium temperatures aside from a weak red emission that quenched above 160 K. The authors attributed this signal to small amounts of oxygen defects resulting from the use of a Bi_2O_3 precursor.^{12,13} To avoid these potential problems, $\text{Cs}_3\text{Bi}_2\text{Br}_9$ was prepared by dissolving BiBr_3 and CsBr in hot, aqueous HBr . Bright yellow powders were collected on cooling through simple vacuum filtration. Thin films were prepared by spin casting a 40 wt% solution of the powder dissolved in dimethylsulfoxide (DMSO). Considering the recent reports that $\text{CH}_3\text{NH}_3\text{PbI}_3$ and other halide perovskites tend to exhibit large concentrations of vacancies in halide sublattice,¹⁴ the as-cast films were subsequently annealed in a Br_2 -rich atmosphere in order to mitigate any influence from defects on the intrinsic optical properties. The annealed films show a significant increase in the diffracted intensity compared with the as-cast films [see Figure 3 (a)], which suggests a substantial improvement to crystal quality with no appreciable change to particle shape or size during the process as demonstrated by the SEM images in Figure 3 (b) and (c).

The X-ray diffraction pattern of the annealed films indicates the crystallites are highly oriented with the (00 l) facets exposed parallel to the plane of the substrate. Films prepared in this way exhibited a strong absorption and, in contrast to previous reports, a weak blue emission at room temperature as shown in Figure 3 (b) and (c). The onset of optical absorption for the films agrees well with the diffuse reflectance data collected on the polycrystalline powder, which shows a direct onset of optical absorption at 2.65 eV (468 nm) (see SI Figure 2). The annealed films display a sharp exciton peak ($\lambda_{max}=440$ nm) when measured in transmission [Figure 3 (b)], similar in shape to features observed in layered organic-inorganic hybrid perovskites.¹⁵⁻¹⁷ To a first approximation,

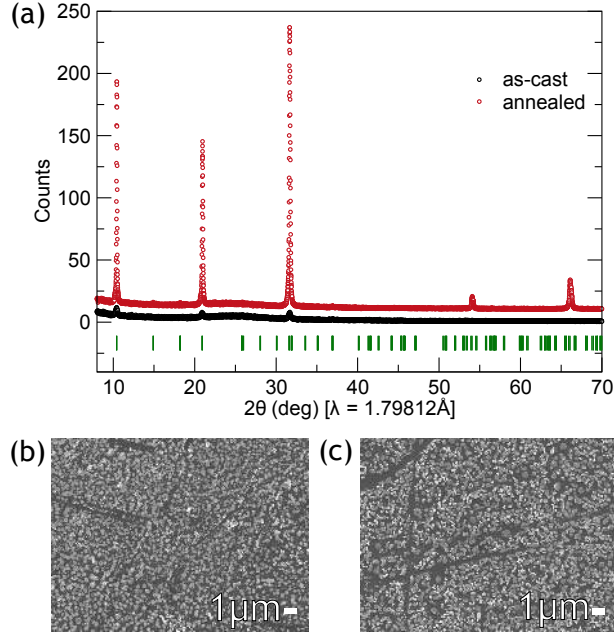


Figure 2: (a) Comparison of the X-ray diffraction patterns for the as-cast (black) films of $\text{Cs}_3\text{Bi}_2\text{Br}_9$ and those annealed in Br_2 atmosphere (red). SEM images of the (b) as-cast and (c) annealed films, showing no change in the morphology of the particles.

the binding energy of the electron-hole pair can be estimated as the difference between the maxima of the exciton peak and the leading edge of the subsequent plateau, which for $\text{Cs}_3\text{Bi}_2\text{Br}_9$ is roughly 940 meV. Compared to the 50 meV exciton binding energy for $\text{CH}_3\text{NH}_3\text{PbI}_3$ ¹⁸ or the 200-300 meV seen for similar layered perovskites,^{19,20} this represents a very strongly localized state that is more commonly found in wide bandgap alkali halides like NaCl.²¹

Although the photoluminescence was very weak, effectively invisible to the naked eye, it still proved possible to resolve five well-defined peaks at 463 nm, 468 nm, 473 nm, 481 nm, and 492 nm [Figure 3 (c)]. It is highly unusual to observe this kind of structured emission at room temperature for non-molecular solids, but is well known to occur at liquid helium temperatures in high purity semiconductors.²² At these low temperatures, the thermal energy available is insufficient to dissociate the electron-hole pair and, as a consequence, the excitons have more time to couple with phonons in the lattice during the recombination process.

As seen from SI Figure 3, the phonon replicas in the emission spectra show no systematic spacing in energy and therefore seem to suggest that the exciton couples to more than one phonon.

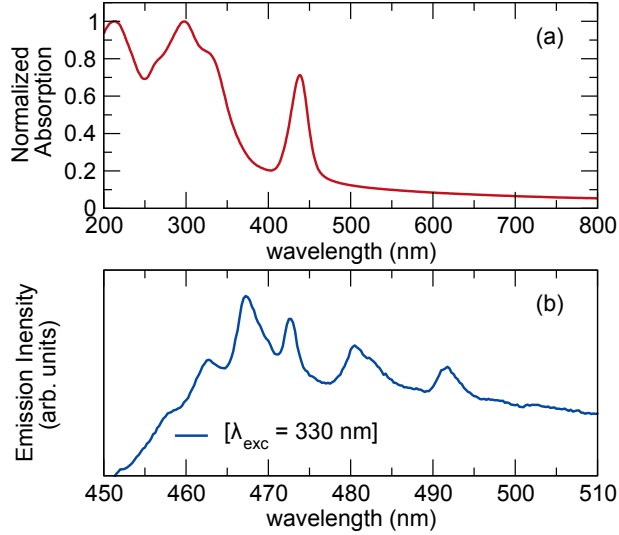


Figure 3: (a) absorption and (b) emission ($\lambda_{exc}=330$ nm) spectra of film of $\text{Cs}_3\text{Bi}_2\text{Br}_9$ after annealing in a Br_2 atmosphere.

Similar luminescent properties have been reported when small concentrations of absorbing ions containing a pair of s^2 electrons (such as Bi^{3+} , Sb^{3+} , or Pb^{2+}) were substituted into non-absorbing matrices like $\text{Cs}_2\text{NaYCl}_6$.²³ In this dilute limit, the vibronic structure was attributed to a pseudo second order Jahn-Teller distortion where the Bi ions shifted away from the center of the regular octahedra to create one short and one long axial bond length.²⁴ These previous reports found several sharp emission lines on top of a broader band, much like in the spectra seen here for $\text{Cs}_3\text{Bi}_2\text{Br}_9$, albeit only at liquid helium temperatures.

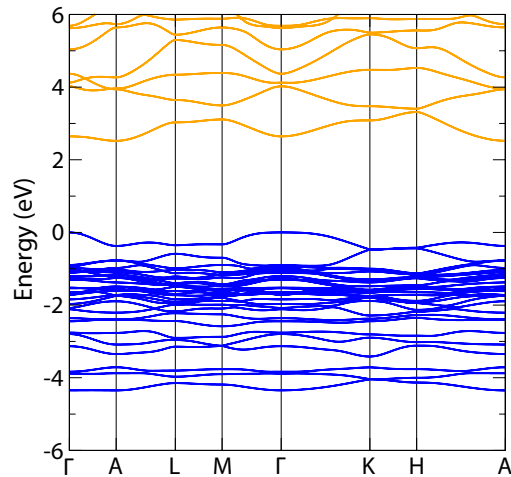


Figure 4: HSE06+SOC DFT band structure of the room temperature form, $P\bar{3}m1$, of $\text{Cs}_3\text{Bi}_2\text{Br}_9$.

Density Functional Theory (DFT) calculations were employed to further elucidate the nature of the electronic excitations. The band structure, shown in Figure 4, reveals the existence of a low lying 2.52 eV indirect transition from the Γ point to A as well as a slightly larger direct gap of 2.64 eV. The shape of the experimental absorption spectra, which is in close agreement with the calculated spectra (see SI Figure 4), suggests that, despite the presence of a lower lying indirect excitation, the primary mechanism for optical excitation occurs at the Γ -point. The weak emission intensity seems consistent with relaxation from the indirect gap and is expected as consequence of the excitons coupling to one or more phonons to emit a photon.

Projecting the atomic orbital character onto the bands reveals that the top of the valence band consists of an admixture of Br 4*p* and Bi 6*s* orbitals with the bottom of the conduction band consisting primarily of Bi *p* (SI Figures 5-8). Thus it appears the excited electron-hole pair is strongly localized on Bi centers in the lattice, and has a pronounced Frenkel (localized) character, rather than the typical Wannier (delocalized) behavior typical of semiconductors.

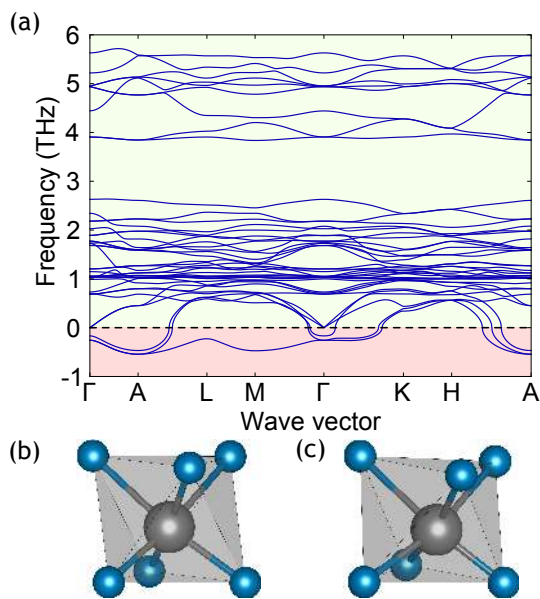


Figure 5: (a) Phonon band structure for the room temperature trigonal structure of $\text{Cs}_3\text{Bi}_2\text{Br}_9$. Local bismuth coordination environment in the room temperature (a) and low temperature (b) structure form of $\text{Cs}_3\text{Bi}_2\text{Br}_9$

The calculated phonon dispersion curve also offers in-sight into why the recombination of the exciton shows the amount of structure that it does. As seen in Figure 5 (a), two soft modes (one

of which is doubly degenerate) associated with a rocking motion of the BiBr_6 octahedra exist at the zone-centre, which suggests the structure is unstable with respect to some energy-lowering structural distortion. This kind of dynamical instability is in keeping with previous temperature-dependent structural studies that identified a phase transition below 95K that distorts the structure into a monoclinic phase.²⁵ The symmetry of these unstable modes (E_g and A_{1u}) are consistent with a distortion from the trigonal to monoclinic form that results from a rocking motion of bromine ions to produce an off-centering of the Bi within the octahedral cage as illustrated in Figure 5 (b) and (c). These E_g and A_{1u} modes are replicated at the zone-boundary at A, but alternating in phase between the layers, further in keeping with the doubled periodicity along c in the monoclinic phase. It, therefore, appears that optical excitation of the films triggers a similar Jahn-Teller distortion of the BiBr_6 octahedra in the same way as was previously observed for isolated Bi ions.²⁴ An imaginary mode of B_g symmetry exists at the zone-boundary q-points M, corresponding to a rotation of the BiBr_6 octahedra about the $[21\bar{1}]$ direction, and L, consisting of the same rotation with alternating phase along c .

Unlike other halide perovskites, $\text{Cs}_3\text{Bi}_2\text{Br}_9$ exhibits unusually strong exciton-phonon coupling. In this aspect, the strongly localized electron-hole pairs created in $\text{Cs}_3\text{Bi}_2\text{Br}_9$ are similar to excitons found in organic chromophores.²⁶ This difference offers a unique counter-example to the weakly bound excitons in $\text{CH}_3\text{NH}_3\text{PbI}_3$ that are easily dissociated into free carriers in photovoltaic cells.²⁷ The unusual optical properties of $\text{Cs}_3\text{Bi}_2\text{Br}_9$ make it an interesting new platform to study the interplay of excitons with lattice vibrations in this new class of light-absorbing materials and offers fundamental insight into how to design new, less-toxic solution processable halide perovskites. In order for materials like $\text{Cs}_3\text{Bi}_2\text{Br}_9$ to find utility in photovoltaic devices, future work will focus on developing structural or compositional modifications that decrease the exciton binding energy and reduce the band gap in order to increase the amount of light collected in the solar spectrum.

Acknowledgements

Computational work in this article used the UCL Legion HPC Facility (Legion@UCL) and the Archer UK National Supercomputing Service, which was accessed through the UK's HEC Materials Chemistry Consortium, funded by EPSRC (EP/L000202). CNS is grateful to the Department of Chemistry at UCL for the provision of a DTA studentship. DOS acknowledges support from the SUPERSOLAR Solar Energy Hub (EP/J017361/1) for the provision of a flexible funding call award and membership of the Materials Design Network.

Supporting Information Available

The diffraction and optical properties of the unannealed films, scanning electron micrographs, direct comparisons between the optical properties of the powder and films, as well as the projected densities-of-state for each elements can be found in the supporting information. This material is available free of charge via the Internet at <http://pubs.acs.org/>.

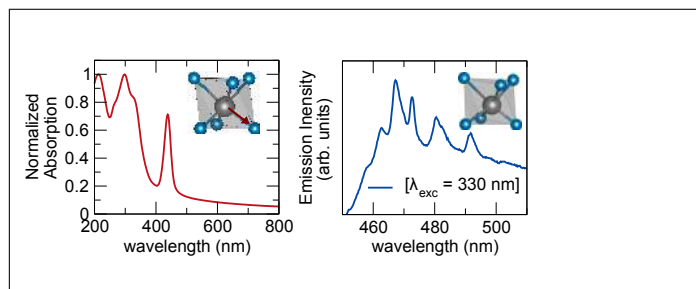
References

- (1) Kojima, A.; Teshima, K.; Shirai, Y.; Miyasaka, T. *Journal of the American Chemical Society* **2009**, *131*, 6050–6051.
- (2) Zhou, H.; Chen, Q.; Li, G.; Luo, S.; Song, T.-b.; Duan, H.-S.; Hong, Z.; You, J.; Liu, Y.; Yang, Y. *Science* **2014**, *345*, 542–546.
- (3) Jeon, N. J.; Lee, H. G.; Kim, Y. C.; Seo, J.; Noh, J. H.; Lee, J.; Seok, S. I. *Journal of the American Chemical Society* **2014**, *136*, 7837–7840.
- (4) Roldan-Carmona, C.; Gratia, P.; Zimmermann, I.; Grancini, G.; Gao, P.; Graetzel, M.; Nazeeruddin, M. K. *Energy Environ. Sci.* **2015**, *8*, 3550–3556.
- (5) Fabini, D. *The Journal of Physical Chemistry Letters* **2015**, *6*, 3546–3548.
- (6) Noel, N. K.; Stranks, S. D.; Abate, A.; Wehrenfennig, C.; Guarnera, S.; Haghighirad, A.-A.; Sadhanala, A.; Eperon, G. E.; Pathak, S. K.; Johnston, M. B.; Petrozza, A.; Herz, L. M.; Snaith, H. J. *Energy Environ. Sci.* **2014**, *7*, 3061–3068.
- (7) Eckhardt, K.; Bon, V.; Getzschmann, J.; Grothe, J.; Wisser, F. M.; Kaskel, S. *Chem. Commun.* **2016**, *52*, 3058–3060.
- (8) Lehner, A. J.; Fabini, D. H.; Evans, H. A.; Hébert, C.-A.; Smock, S. R.; Hu, J.; Wang, H.; Zwanziger, J. W.; Chabynyc, M. L.; Seshadri, R. *Chemistry of Materials* **2015**, *27*, 7137–7148.
- (9) Lehner, A. J.; Wang, H.; Fabini, D. H.; Liman, C. D.; Hébert, C.-A.; Perry, E. E.; Wang, M.; Bazan, G. C.; Chabynyc, M. L.; Seshadri, R. *Applied Physics Letters* **2015**, *107*.
- (10) McClure, E. T.; Ball, M. R.; Windl, W.; Woodward, P. M. *Chemistry of Materials* **2016**, *28*, 1348–1354.

- (11) Slavney, A. H.; Hu, T.; Lindenberg, A. M.; Karunadasa, H. I. *Journal of the American Chemical Society* **2016**, *138*, 2138–2141.
- (12) Timmermans, C. W. M.; Blasse, G. *Phys. Status Solidi B* **1981**, *106*, 647–655.
- (13) Timmermans, C.; Blasse, G. *Journal of Luminescence* **1981**, *24-25*, 75–78.
- (14) Walsh, A.; Scanlon, D. O.; Chen, S.; Gong, X. G.; Wei, S.-H. *Angewandte Chemie* **2015**, *127*, 1811–1814.
- (15) Dohner, E. R.; Jaffe, A.; Bradshaw, L. R.; Karunadasa, H. I. *Journal of the American Chemical Society* **2014**, *136*, 13154–13157.
- (16) Park, B.-W.; Philippe, B.; Zhang, X.; Rensmo, H.; Boschloo, G.; Johansson, E. M. J. *Advanced Materials* **2015**, *27*, 6806–6813.
- (17) Ahmad, S.; Kanaujia, P. K.; Beeson, H. J.; Abate, A.; Deschler, F.; Credgington, D.; Steiner, U.; Prakash, G. V.; Baumberg, J. J. *ACS Applied Materials & Interfaces* **2015**, *7*, 25227–25236.
- (18) Miyata, A.; Mitioglu, A.; Plochocka, P.; Portugall, O.; Wang, J. T.-W.; Stranks, S. D.; Snaith, H. J.; Nicholas, R. J. *Nature Physics* **2015**, *11*, 582–587.
- (19) Cheng, Z.; Lin, J. *CrystEngComm* **2010**, *12*, 2646–2662.
- (20) Mitzi, D. B.; Chondroudis, K.; Kagan, C. R. *Inorganic Chemistry* **1999**, *38*, 6246–6256.
- (21) Williams, R. T.; Kabler, M. N. *Physical Review B* **1974**, *9*, 1897–1907.
- (22) Kovalev, D.; Averboukh, B.; Volm, D.; Meyer, B. K.; Amano, H.; Akasaki, I. *Phys. Rev. B* **1996**, *54*, 2518–2522.
- (23) Van Der Steen, A. C.; Dirksen, G. J. *Chemical Physics Letters* **1978**, *59*, 110 – 112.

- (24) Blasse, G. In *Electronic and Vibronic Spectra of Transition Metal Complexes I*; Yersin, H., Ed.; Springer Berlin Heidelberg, 1994; Chapter Vibrational structure in the luminescence spectra of ions in solids, pp 1–25.
- (25) Ivanov, Y.; Sukhovskii, A.; Lisin, V.; Aleksandrova, I. *Inorganic Materials* **2001**, *37*, 623–627.
- (26) Gregg, B. A.; Hanna, M. C. *Journal of Applied Physics* **2003**, *93*, 3605–3614.
- (27) Herz, L. M. *Annual Review of Physical Chemistry* **2016**, *67*.

Graphical TOC Entry



The unusual electronic structure of $\text{Cs}_3\text{Bi}_2\text{Br}_9$ produces a sharp exciton peak in the absorption spectra with a binding energy that was approximated to be 940 meV, which is substantially stronger than values found in other halide perovskites and, instead, closely reflects the behavior of alkali halide crystals.